The Cryosphere Discuss., 8, 5321–5360, 2014
www.the-cryosphere-discuss.net/8/5321/2014/
doi:10.5194/tcd-8-5321-2014

The Cryosphere Discussions

Paleo-ice flow directions of the Northern Antarctic Peninsula ice sheet based upon a new synthesis of seabed imagery

C. Lavoie[1,2], E. W. Domack[3], E. C. Pettit[4], T. A. Scambos[5], R. D. Larter[6], H.-W. Schenke[7], K. C. Yoo[8], J. Gutt[7], J. Wellner[9], M. Canals[10], J. B. Anderson[11], and D. Amblas[10]

[1]Istituto Nazionale di Oceanografia e di Geofisica Sperimentale (OGS), 34010 Borgo Grotta Gigante, Sgonico, Italy
[2]CESAM/Department of Geosciences, University of Aveiro, Aveiro, 3810-193, Portugal
[3]College of Marine Science, University of South Florida, St. Petersburg, Florida, 33701, USA
[4]Department of Geosciences, University of Alaska Fairbanks, Fairbanks, Alaska, 99775, USA
[5]National Snow and Ice Data Center, University of Colorado, Boulder, Colorado, 80309, USA
[6]British Antarctic Survey, Cambridge, Cambridgeshire, CB3 0ET, UK
[7]Alfred Wegener Institute, Helmholtz Centre for Polar and Marine Research, Bremerhaven, 27568, Germany
[8]Korean Polar Research Institute, Incheon, 406-840, South Korea
[9]Department of Earth and Atmospheric Sciences, University of Houston, Houston, Texas, 77204, USA

[10]Departament d'Estratigrafia, Paleontologia i Geociències Marines, Universitat de Barcelona, Barcelona, 08028, Spain
[11]Department of Earth Science, Rice University, Houston, Texas, 77251, USA

Received: 13 September 2014 – Accepted: 26 September 2014 – Published: 15 October 2014

Correspondence to: C. Lavoie (clavoie@ua.pt) and E. W. Domack (edomack@usf.edu)

Published by Copernicus Publications on behalf of the European Geosciences Union.

Abstract

We present a new seafloor map for the northern Antarctic Peninsula (AP), including swath multibeam data sets from five national programs. Our map allows for the examination and interpretation of Last Glacial Maximum (LGM) paleo-ice sheet/stream flow directions developed upon the seafloor from the preservation of: mega-scale glacial lineations, drumlinized features, and selective linear erosion. We combine this with terrestrial observations of flow direction to place constraints on ice divides and accumulation centers (ice domes) on the AP continental shelf. The results show a flow bifurcation as ice exits the Larsen-B embayment. Flow emanating off the Seal Nunataks (including Robertson Island) is directed toward the southeast, then eastward as the flow transits toward the Robertson Trough. A second, stronger "streaming flow" is directed toward the southeast then southward, as ice overflowed the tip of the Jason Peninsula to reach the southern perimeter of the embayment. Our reconstruction also refines the extent of at least five other distinct paleo-ice stream systems which, in turn, serve to delineate seven broad regions where contemporaneous ice domes must have been centered on the continental shelf during the LGM time interval. Our reconstruction is more detailed than other recent compilations because we followed specific flow indicators and have kept tributary flow paths parallel.

1 Introduction

The reconstruction of paleo-ice sheets/stream flow directions depends first upon an accurate assessment of accumulation centers, ice divides, and flow paths (outlets) (Andrews, 1982). Studies of the configuration of the Antarctic Peninsula Ice Sheet (APIS) during the Last Glacial Maximum (LGM; time interval ~ 23–19 kyr BP) suggest that the grounded ice reached the continental shelf break (e.g. Larter and Barker, 1989; Banfield and Anderson, 1995; Larter and Vanneste, 1995; Wellner et al., 2001; Canals et al., 2002; Evans et al., 2005; Heroy and Anderson, 2005; Amblas et al.,

2006; Wellner et al., 2006; Simms et al., 2011). The seafloor of the Antarctic Peninsula (AP) continental shelf is characterized by over-deepened troughs and basins where mega-scale glacial lineations (MSGLs) (Clark, 1993; Clark et al., 2003) and large-scale flowlined bedforms such as glacial flutes, mega-flutes, grooves, drumlins and crag-and-tails provide geomorphic evidence for former regional corridors of fast-flowing ice and drainage directions of the APIS on the continental shelf. Also of importance is their synchroneity as the ice flows change during the ice sheet evolution, from ice sheet to ice stream to ice shelf (Gilbert et al., 2003; Dowdeswell et al., 2008).

Our capability to image specific flow directions and styles on the Antarctic continental shelf is critical to any glacial reconstruction in so much as they help us to understand the present and future ice sheet's behavior. Recently, Livingstone et al. (2012) published an inventory of evidence for paleo-ice streams on the continental shelf of Antarctica at LGM. Their reviews are in agreement with previous studies and highlight that the West (Pacific) AP continental shelf is characterized by preferred regional ice flow pathways on the middle shelf through cross-shelf troughs connected to major flow paths on the outer shelf (e.g. Evans et al., 2004; Heroy and Anderson, 2005). On the other side, the East (Weddell Sea) AP continental shelf is less well defined but characterized by multiple deep tributaries on the inner shelf that converge in shallow troughs on the mid to outer shelf (e.g. Evans et al., 2005). Nevertheless, our knowledge on the accumulation centers, ice divides and flow paths at the LGM time interval, such as in the Larsen-B embayment, is limited and particularly relevant to the APIS reconstruction, where the broad continental shelf served as a platform for extension of the glacial systems that spilled off the Detroit and Bruce Plateau ice caps. In fact the AP is believed to have experienced the largest percentage change in areal extent of glacial cover of any sector of the Antarctic margin through the last glacial cycle (i.e. MIS stage 2 to 1). For instance our reconstruction shows that the current APIS covers ~ 23 % of the total area of grounded ice coverage at LGM. The APIS system in particular is a significant bellwether system in the evolution of the Antarctic Ice Sheet because it is:

Discussion Paper | Discussion Paper | Discussion Paper | Discussion Paper |

1. the one system today that is most closely tied to surface driven ablation and accumulation changes, having equilibrium lines a.s.l. as a consequence of significantly warm summer temperatures;
2. exposed to a contrasting oceanographic regime of cold and warm water on the eastern and western sides, respectively, and
3. the most northern of the ice sheet systems and it is exposed to southward excursions in westerly winds and the Antarctic Circumpolar Current.

In this paper, we enhance our knowledge on the paleo-ice sheet/stream flow drainage directions of the APIS based upon a new synthesis of single and swath bathymetry data, and provide a comprehensive assessment of the flow paths, ice divides and accumulation centers pertaining to the glacial history of the northern APIS at the LGM time interval. The spatial coverage of the bathymetric data is extensive (Fig. 1) and for this and the above reasons we focus upon regional systems by dividing it into seven sectors. These include the (1) Larsen-B embayment, (2) Larsen-A and James Ross Island, (3) Joinville Archipelago Platform, (4) Bransfield Strait, (5) Gerlache–Croker–Boyd Straits, (6) Palmer Deep and Hugo Island Trough, and (7) Biscoe Trough. We draw upon our compiled seabed map the geomorphic features that define the specific flow paths at LGM and glacial tributaries across the inner to outer shelf to infer the flow paths, ice divides and the accumulation centers that controlled the APIS flow drainage and subsequent retreat history. Finally, we discuss the characteristics of the reconstructed northern APIS and its regional significance for ice sheet modeling.

2 Methods

2.1 Data sets

Extensive multibeam swath bathymetry data have been acquired from regions recently uncovered by the collapse of the Larsen Ice Shelf system. Ice-flow directions within

the Larsen-B embayment are indicated by a series of interconnected (1) multibeam surveys beginning with a United States Antarctic Program (USAP) program in 2000 including work by the British Antarctic Survey (2002), additional USAP surveys (2001 and 2006), Alfred Wegener Institute, Helmholtz Centre for Polar and Marine Research surveys (2009 and 2011) and Korea Polar Research Institute survey (KOPRI, 2013) under the LARISSA project, and (2) single beam sonar data from USAP in 2005. Detailed observations of the seafloor morphology in the Larsen-A embayment, the area surrounding James Ross Island and offshore from Joinville Archipelago were collected by the USAP program between 2000–2002, 2005–2007, in 2010 and 2012 including work by the British Antarctic Survey (2002) and UK Hydrographic Office (2006–2008). The Bransfield Strait has been covered by the Spanish Antarctic program between 1991 and 1997, USAP program (1995–1997, 1999–2002, and 2005–2011) and UK Hydrographic Office (2006–2008, 2010 and 2012). The multibeam swath bathymetry data from the Gerlache–Croker–Boyd Strait, Palmer Deep and Hugo Island Trough, and Biscoe Trough are from the Spanish Antarctic program in 1996–1997 and 2001–2002, the USAP program (1995–1997, 1999–2002, and 2005–2012) and KOPRI (2013). The data set was gridded at a cell size of 30 m × 30 m and analyzed with illumination at variable azimuths. Furthermore, single beam sonar data from NGDC Marine Trackline Geophysical database (http://ngdc.noaa.gov/mgg/geodas/trackline.html) were used to support the delimitation of the continental shelf ice domes.

2.2 Bedform mapping

We assume that our flow lines reconstructions are contemporaneous to the LGM time interval considering that our observed seafloor lineations over resistant substrate were carved last by the APIS at LGM, although their formation may derive from previous over time-integrated glacial processes. From the observed seafloor lineations, central flow lines were established at the root of all major glacier tributaries adjacent to areas of reasonable coverage in the multibeam data. These central flow lines were preserved along the path by forcing tributary contributions to remain parallel and consistent with observed seafloor lineations. In this way converging flow can be evaluated more easily than by using "idealized" single-line flow arrows (as has been done on previous reconstructions). The number of lines in a given flow path is defined by the number of tributaries, and is only a visual approximation of the ice discharge for that flow path. In some cases, ice flow across the seafloor diverged around obstacles but remained parallel within the larger confining troughs or fjords. Small-scale basal-flow divergence patterns such as these were not preserved in our reconstruction.

The orientation of the bedrock striations at Cape Framnes and Foyn Point (Larsen-B embayment; Fig. 2) were measured with a Brunton Compass, corrected for regional declination, and compared to visual data of large-scale bedrock fluting from overflights during 2010 (USAP-ship based helicopters during LARISSA NBP10-01 cruise).

2.3 Ice volume estimation and assumptions

We utilize two different algorithms to estimate volumes of the ice sheet, depending upon the type of system, ice domes or streaming flow. For the domes in this reconstruction, we use a simple, radially symmetric, Bodvarsson–Vialov model as presented in Bueler et al. (2005). This model assumes the shallow-ice approximation (no sliding bed) and Glen-type ice flow with a softness that depends on the average temperature. The model can directly predict the thickness as a function of distance from the dome center ($r = 0$) as:

$$H(r) = \left(2^{(n-1)}\frac{\dot{b}}{\Gamma}\right)^{1/(2n+2)} \left(L^{1+1/n} - r^{1-1/n}\right)^{n/(2n+2)} \quad (1)$$

$$\Gamma = \frac{2A(\rho g)^n}{n+2} \quad (2)$$

where H is the ice thickness, $\dot{b}$ is the accumulation rate, L is the lateral extent of the ice dome, assuming it is circular, and $n = 3$ for typical Glen-type ice flow. Γ is a parameter that depends on the ice softness, A, which is temperature dependent, the density (ρ)

of ice, and gravity (g). We are assuming that the same strongly orographic precipitation occurred during LGM interval as today, and the ice temperature was around 0 °C (mostly temperate) for the West AP domes and averaging −10 °C for the domes located on the East side (see Sect. 4.3). We based the minimum and maximum on a low-end and high-end approximation of the accumulation rates, respectively. In these accumulations rate assumptions, we took into account that some domes are more exposed to the prevailing storm direction and some will be in the lee, resulting higher or lower accumulation rates.

To estimate the ice volume of the convergent flow paths we use less established assumptions. The average depths along the flow paths are estimated from our swath bathymetry map and the IBCSO map gridded at 500 m (Arndt et al., 2013). For the minimum volumes, we assume that the ice streams were lightly grounded until the shelf break or to the end of the defined flow path (except for Larsen-B/Jason Trough) where the ice thickness must be about 10 % more than the average depth to prevent flotation (allowing to the deepest areas to be subglacial lakes, rather than full of ice). We assume a minimal surface slope (0.001) similar to the lowest sloping modern ice streams. For the maximum volumes, we assume that the ice was grounded until the continental shelf break (except for Larsen-B/Jason Trough). We assume the surface slope of the ice was steeper (0.005), but not too steep to exceed the nearby ice dome elevations. In both estimations, it will depend on the geology. A softer more malleable bed would have a lower profile ice stream (but it still needs to be thick enough to be grounded), a stiffer bed would require a slightly steeper profile.

3 Results

3.1 Larsen-B embayment

The major collapse of the Larsen-B Ice Shelf in 2002 (Scambos et al., 2003), unprecedented in the Holocene history of this glacial system (Domack et al., 2005; Curry and

Discussion Paper | Discussion Paper | Discussion Paper | Discussion Paper |

Pudsey, 2007), has provided a unique opportunity for seafloor mapping. This work reveals a far more detailed flow pattern in Larsen-B embayment than that inferred by general orientation of bathymetric troughs derived from sparse swath or single line bathymetric data. Such earlier approaches suggested that all Larsen-B ice flowed out toward the Robertson Trough (e.g. Evans et al., 2005; Davies et al., 2012; Livingstone et al., 2012).

By using more a more detailed analysis of flow indicies available from the swath data we now recognize two distinct flow trajectories that split the Larsen-B embayment into two outlets (Fig. 2). The first relates to the attenuated drumlinized bedforms and highly attenuated MSGLs observed in the northern perimeter of the Larsen-B embayment. The ice flow emanating off the Seal Nunataks and Robertson Island directed flow toward the southeast then eastward as the flow transits toward the Robertson Trough, a feature that connects Larsen-A and B (Evans et al., 2005). This flow pattern extends across relatively shallow depths of less than 500 m and was fed by indistinct tributary confluence.

In contrast, the southern perimeter is marked by stronger “streaming flow” indicators fed by large tributaries draining the APIS, including the Crane Glacier and most likely the Evans, Green and Hektoria Glaciers. The well-defined drumlinized bedforms with crescentric scour and MSGLs indicate that ice flow was funneled into the Cold Seep Basin (Fig. 3a) and moved toward the southeast from the interior. From the edge of the SCAR Inlet (Larsen-B Ice Shelf), the swath bathymetric map shows evidence of a northeastward flow (Fig. 3b) that downstream shifted toward the southeast, thus convergent with the flow streaming from the Cold Seep Basin corridor. The SCAR Inlet ice stream system was fed by the tributaries of the Starbuck, Flask, and Leppard Glaciers. Our flowlined bedform compilation suggests that the southeastward flow in the southern perimeter of the Larsen-B changed to a southward direction with ice overflowing the tip of the Jason Peninsula, offshore the northern region of the Larsen-C Ice Shelf (Figs. 2 and 3c), to reach the Jason Trough. This southward flow orientation is

supported by bedrock striations and flute orientations SSW at Cape Framnes, Jason Peninsula (Fig. 4) that parallel marine flow indicies found directly offshore.

Finally, the southernmost swath bathymetry data at the edge of the northern Larsen-C Ice Shelf indicates a southeastward ice flow orientation on a seafloor deeper than 400 m. Recent seismic reflection soundings close to the northern ice shelf front and inward the shipboard surveys show a uniform water cavity thickness beneath the ice shelf of around 220 to 240 m (Brisbourne et al., 2014).

3.2 Larsen-A and James Ross Island

Our mapped flow pattern of the Larsen-A and James Ross Island sector differs only in fine detail to those of earlier reconstructions (e.g. Evans et al., 2005; Johnson et al., 2011; Davies et al., 2012). The evidence is the establishment of two major outlets: the Robertson Trough system and the Erebus–Terror system (Fig. 5). The Robertson Trough system collected flow out of the Larsen-A, southern Prince Gustav Channel, and portions of Admiralty Sound. The ice flowed from the Larsen-A, derived mainly from the Detroit Plateau (AP), toward the south, then east. It then coalesced with the southern Prince Gustav Channel flow across the shelf toward the southeast and finally directly east (Pudsey et al., 2001; Gilbert et al., 2003; Evans et al., 2005). On the outer shelf the ice flow coalesced with the northern perimeter of the Larsen-B flow to form a major ice flow trend in the Robertson Trough.

The Erebus–Terror system captured flow out of the northern Prince Gustav Channel, Antarctic Sound, and Admiralty Sound. The northern Prince Gustav Channel, shows evidence of a main eastern flow direction, fed by tributaries from ice caps on Trinity Peninsula and James Ross Island before coalescing with the Antarctic Sound and the Admiralty Sound flows into the Erebus and Terror Gulf to reach the shelf break. Flow within the Prince Gustav Channel was separated from the south Larsen-A system by an ice divide, as a consequence of an ice saddle (divide) that extended from the Detroit Plateau across the James Ross Island (Camerlenghi et al., 2001). Recent observations and cosmogenic isotope exposure-age dating on erratic boulders on James

Discussion Paper | Discussion Paper | Discussion Paper | Discussion Paper |

Ross Island by Glasser et al. (2014) suggest that the ice divide that crosses the central Prince Gustav Channel may be only developed during the post-LGM recession.

3.3 Joinville Archipelago Platform

The platform surrounding the northernmost extension of the AP terrain (D'Urville, Joinville, and Dundee Islands) has very limited multibeam coverage. Only two distinctive troughs have been imaged and flow lines are conjectural and defined (as in earlier approaches) by recognition of bathymetric troughs. Portions of the flow out of the Larsen Channel, between D'Urville Island and Joinville Island, and out of the unnamed channel between Joinville Island and Dundee Island ran in a southwestern direction coalescing with the Antarctic Sound flow to the Erebus–Terror system. The other portion shows evidence of east and southeast flows. South of Joinville Island, the multibeam data imaged drumlin-like features indicating that ice was grounded on the Joinville Plateau, indicating that the APIS extended across the shelf (Smith and Anderson, 2011; their Fig. 6).

3.4 Bransfield Strait

The continental shelves off the Trinity Peninsula (e.g. Lawver et al., 1996; Canals et al., 2002) and the South Shetland Islands (Simms et al., 2011) reveal paths of paleo-ice streams that drained into the Bransfield Strait. The depth of the Bransfield Strait (greater than 1000 m) necessitates that grounded ice flow transitioned to an ice shelf (floating glacier ice that was not in contact with the seafloor). This system must have been confined to the Bransfield basin between tributary flow out of the Orleans Strait, off the Trinity Peninsula, and the South Shetland Islands (Fig. 5). As indicated by the curvature of bedforms on the surface of the fans (i.e. Maxwell Bay and Admiralty Bay) and major troughs (i.e. Lafond, Laclavere and Mott Snowfield) that extend into Bransfield Strait, flow of the ice shelf was conjectured to involve a northeastern direction more or less parallel to the trend of the basin (Canals et al., 2002; Willmott et al., 2003; Heroy

et al., 2008). Outlets in the eastern portions of the basin are even less well defined but must have involved partitioned grounded flow out across the northern end of the South Shetland Platform (just northeast of King George Island), out beyond Elephant Island, and into the Powell Basin (Fig. 6).

3.5 Gerlache–Croker–Boyd Straits

In the Gerlache–Croker–Boyd Straits, the streaming ice flow is confined in a spectacular bundle structure of 100 km long and flowing to the north northwest (Canals et al., 2000). Almost the entire ice drainage out of the Gerlache Strait was funneled through the Croker Passage which included glaciers draining the eastern side of Anvers and Brabant island and the western flank of the Bruce and Dyer plateaux (Evans et al., 2004). These tributary systems converged at various depths (submarine hanging valleys) where fjord valleys joined the Gerlache Strait and the Croker Passage. This along with the large number of tributaries requires considerable constriction of flow lines within the Croker Passage outlet path (Fig. 5). Some tributaries are added as the system flows out toward the shelf break, beyond Smith Island and this maintains the tight, parallel arrangement of flow in the Boyd Strait. However, at the shelf break the grounding line system clearly shows a spread of flow trajectories out toward the shelf break (Canals et al., 2003; their Fig. 2b).

3.6 Palmer Deep and Hugo Island Trough

The outflow from the Palmer Deep and Hugo Island Trough is one of three major tributary systems that terminate as an outlet system along the western Antarctic Peninsula continental shelf edge (Fig. 5). These were delineated first by Pudsey et al. (1994), Vanneste and Larter (1995) and later outlined in detail by Domack et al. (2006). The systems include tributary glaciers from the Graham Land Coast, the Flandres Bay and Bismark Strait and ice which flowed out of Dallmann Bay around the northwest corner of Anvers Island (Fig. 5). In Graham Land Coast the ice flow emanating from the fjords directed flowed to the northeast coalescing with the Palmer Deep ice flow in Hugo Island Trough and crossed the mid-shelf in a northern direction to the outer shelf (Domack et al., 2006). On the outer shelf the ice flow coalesced with the Dallman Bay flow that runs out from Anvers Island and Brabant Island.

3.7 Biscoe Trough

The cross-shelf Biscoe Trough system consists of three branches with up to 800 m overdeepened troughs, a topographic ridge up to 300 m high crosses the main branch in a southwest and northeast direction, and a smoother surface toward the shelf edge at 400–500 m depth (Canals et al., 2003; Amblas et al., 2006). The flowlined bedforms show a general converging westward flow directions toward the shelf edge. Biscoe Trough system also shows a spread of flow trajectories out toward the shelf break. This system was fed by ice flow primarily off Renaud Island archipelago but notably, as well, contains clear indications of ice flow off mid to outer shelf banks with a distinct flow divide out along the trend defined by Hugo Island.

4 Interpretation and discussion

Based upon the above observations we recognized six major outlets for paleo-ice streams drainage off the APIS during the LGM and refined the locations of their ice divides (Fig. 5). In addition, the patterns revealed by our flow directions reconstruction indicate the locations and areal dimensions of at least seven major ice domes centered on the middle to outer AP continental shelf. Below we focus on a comprehensive interpretation of the new seabed morphology and discuss their regional implications regarding flow paths, ice divides and centers of accumulation.

4.1 Flow bifurcation in Larsen-B embayment

Our observations of streamed bedforms in the Larsen-B embayment indicate that the modern glaciers (i.e. Crane, Leppard, and Flask Glaciers) were not tributaries of the Robertson mid-outer shelf paleo-ice stream as previously interpreted by Evans et al. (2005) and highlighted in previous reviews (e.g. Davies et al., 2012; Livingstone et al., 2012; Ó Cofaigh et al., 2014). We provide two possible explanations to explain the flow divergence we observe in the Larsen-B embayment. Although, there are no surface expressions of seismic stratigraphic boundaries on the shelf interpreted as a LGM ice stream bifurcation (Smith and Anderson, 2009), the first explanation is based on the hypothesis of a non-uniform geological framework. The diverging flow could be explained by the southeastward extension of the Seal Nunatak and Robertson Island post-Miocene volcanic sequence, in contact with Mesozoic rocks in the Larsen embayment. We infer from scanty seismic data the presence of Mesozoic mudrocks similar to the Nordensköld Formation (Jurassic black shale; Reinardy et al., 2011) and Cretaceous sedimentary sequences of Roberston Island. These are known to have influenced bed deformation within tills derived from them (Reinardy et al., 2011). One hypothesis, therefore, would suggest that the divergence of flow was related to faster flow that followed and was funneled out of the inner Larsen-B embayment by a bed that was more easily deformed (mud base) than the higher friction of the sandy volcaniclastic palagonite units that comprise the Seal Nunatak massif. Detailed petrographic analysis of the respective tills could test this hypothesis.

The second hypothesis to take into consideration relates to pre-determined topography and glacial dynamics that could have split the flow direction on the mid-shelf. The existence of a slightly elevated seabed over the middle shelf could have acted as a barrier between the Robertson Trough and Jason Trough diverging flow. Unfortunately, this hypothesis cannot be reliably tested at this time because heavy ice cover during the austral summer makes navigation and acquisition of key swath bathymetry very difficult. However, some bathymetric data and seismic profiles from shipboard surveys south of Jason Peninsula (Sloan et al., 1995) show evidence of shallow shelf banks at less than 300 m water depth – these could have acted as a topographic prow dividing the acting on glacial flow (Fig. 5). The examination of a time-series of MODerate-resolution Imaging Spectroradiometer (MODIS) images from the northeastern Antarctic Peninsula shows unequivocal evidence of several previously unknown reef and shoal areas, based on their influence on sea ice drift and grounding of small icebergs (Table 1, Figs. 7 and S1, and Video S2 in the Supplement; see also http://nsidc.org/data/iceshelves_images/index_modis.html). In the 12 year series of images, shoal areas appear as frequent stranding areas of sea ice and small icebergs, particularly during heavy winter sea ice pack periods. Larger icebergs (having 200–350 m keels) show drift paths strongly controlled by the shoals. Stranding of sea ice (especially for the informally named Bawden, Roberston, and Jason shoal or reef areas, see Table 1) indicates the shallowest areas of the region. These high areas could have served as centers of glacial nucleation similar to the model proposed for shallows across the Bellingshausen Sea continental shelf (Domack et al., 2006).

The above explanations could have interacted to cause the divergence of the flow observed within the Larsen-B embayment; a combination of two processes: deformation of weak bed material and bifurcation of the ice around a topographic high. Divergence of flow lines have been already observed at the margin of the Greenland Ice Sheet and Antarctica. A modern example that shows fast flowing ice bifurcation can be observed on the flow velocity field map of the northeast Greenland Ice Stream, the southern flow feeds Storstrømmrn and the northern flows the outlet glaciers of Zachariæ Isstrøm and Nioghalvfjerdsfjorden (Joughin et al., 2001, 2010). According to Knight et al. (1994) a topographic obstacle of about 400 m high is sufficient to impose a pattern of ice divergence. Modern analogs such as Siple Dome show diverging flow of marine-based ice streams (bed 600 to 700 m b.s.l. – below sea level) around a topographic high only 300 to 400 m b.s.l. (Fretwell et al., 2013). In the Siple Coast region, only 200 to 300 m topographic different is sufficient to create diverging flow separated by ice domes.

4.2 Evidence of ice divides

An ice divide is the boundary at greatest altitude separating opposite ice flow directions which defines ice drainage systems, analogous to a water divide. The major center of radial flow in the northern AP at LGM was the separation of the West and East AP along the Bruce and Detroit Plateaux on the Trinity Peninsula. Our results suggest that the northern AP was bounded by secondary ice divides interconnected with the main center (Fig. 5). In order to explain our East AP flow line reconstruction, ice divides must have included the following: (1) from the AP across the Seal Nunatak and Robertson Island to divide the ice flow between the NE Larsen-B embayment and the western area of Larsen-A, (2) from the Bruce Plateau (AP) to Cape Longing to divide flows between Larsen-A and southern Prince Gustav Channel, (3) from the Detroit Plateau (AP) SE across the Prince Gustav Channel and up across the center of James Ross Island (Camerlenghi et al., 2001) before continuing across Admiralty Sound and Seymour Island to split the ice flow between the southern and northern Prince Gustav Channel, dividing the ice flow on James Ross Island and Admiralty Sound. Moreover, a flow divide must have bridged the Trinity Peninsula to the Joinville Island Group, and run along the axis of D'Urville Island, across the Larsen Channel, Joinville Island and Dundee Island (4) according to the seabed morphology in the Antarctic Sound.

On the West AP, the flow divides are defined by: (1) the South Shetland archipelago, (2) a boundary that runs from the AP across the Orleans Strait, Trinity Island and along a series of shelf banks at the western end of the Bransfield Strait that divide the ice flow between the Bransfield Strait and Gerlache–Boyd Strait, (3) a line running from the Bruce Plateau (AP) across Gerlache Strait, Wiencke Island, southern edge of Anvers Island, Schollaert Channel and up along the crest of Brabant Island to explain the constriction of flow lines in the Gerlache Strait, and (4) flow divides must have been present on the Anvers Island and Renaud Island to explain the Palmer Deep and Hugo Trough ice flow system and its separation from the Biscoe Trough.

Once ice becomes thick enough to overtop a bedrock divide, the divide will be determined by the accumulation rate pattern and the dynamics of ice flow. These divides are not stationary and can evolve under variations in climate or boundary condition (e.g. Nereson et al., 1998; Marshall and Cuffey, 2000). Indeed, an entire ice dome can change shape as climate conditions changes on a timescale of a few hundred to thousands of years, depending on the accumulation rate and size of the divide (Nereson et al., 1998; Marshall and Cuffey, 2000).

4.3 Inferred ice domes on the continental shelf

Pioneering studies show two separate ice domes, one covering the northern AP and the other upon the South Shetland Islands (Banfield and Anderson, 1995; Bentley and Anderson, 1998). Our paleo-ice flow reconstruction indicates the extent of at least six distinct paleo-ice stream systems across the northern AP continental shelf and these must serve also to delineate at least seven broad regions where ice domes must have been centered, out on the continental shelf. The presence of the domes is required to constraint lateral spreading of each of the paleo-ice stream outlets. We define each of these features here by assigning names associated with the nearest prominent headland for each ice cap, headlands which likely provided some axial orientation to the cap divide. These include: Hugo Dome, Marr Dome, Brabant Dome, Livingston Dome, Snow Hill Dome, Robertson Dome, and Hektoria Dome (Fig. 5).

The exact dimensions and character of each of these domes is difficult to define because these areas of the continental shelf are generally devoid of multibeam coverage. Further, extensive iceberg scouring across these banks has largely obscured original glacial flow indicators, which might have provided some sense of paleo-ice flow direction. Nevertheless, some small troughs and lineated features do exist, for at least three of the inferred domes, and these do contain flow indicators. For the Marr, Brabant and Livingston Domes, some radial flows can be seen in the orientations found in small troughs that drain the mid-point divides, in about the middle of the continental shelf (Fig. 5). Further, the Hugo Dome can be seen to have directed flow into the Biscoe

Trough from a position considerably out on the continental shelf. Here the flow lines actually flow back toward the Peninsula for a distance (Amblas et al., 2006; their Fig. 5). Hence, this limited evidence does indicate that the mid-shelf hosted centers of ice accumulation (Fig. 5). In this hypothesis the continental-shelf ice domes do not necessarily require excessive elevation, only sufficient height to have grounded the system and allowed each dome to constrain the surrounding paleo-ice streams. Our hypothesis for these ice domes is not without precedent as some work on the East Antarctic margin has postulated a similar situation, where major divides were diverted and constrained by large ice domes that rested upon shelf banks (Eittreim et al., 1995). Also an independent ice cap persisted on Alexander Island, western Antarctic Peninsula, through the LGM and deglaciation (Graham and Smith, 2012). Furthermore, there are existing modern ice domes that separate fast flowing, marine-based ice in West Antarctica, including Siple Dome (surface elevation 600 m a.s.l. and an ice thickness of 1000 m; Gades et al., 2000; Conway et al., 2002).

The seaward extent of each of these domes would seem to correspond to the outer continental shelf, as outlet systems are uniformly constrained out to the grounding line position (the outer shelf) in each of the systems we examined. The exception to this is the broad apron of the grounding line associated with the Gerlache–Croker–Boyd Strait and Biscoe ice streams. In those cases diverging flow is clearly imaged out across the continental shelf break, indicating spreading flow toward the grounding line. Indeed, the extensive relief of Smith Island (maximum elevation 2100 m) would likely have blocked any ice flow associated with the Brabant Dome from reaching the outermost shelf (Fig. 5). This spreading flow is similar to that observed for unrestricted paleo-ice stream fans such as in the Kveithola Trough off Svalbard (Rebesco et al., 2011).

While the areal dimensions of the ice domes are fairly certain, their thickness is less well defined. We can assume that these features were thick enough to have served as effective lateral constraints to ice stream outlets and to have allowed the dome to have been grounded across a bathymetry of approximately 350 m, on average. The

Discussion Paper | Discussion Paper | Discussion Paper | Discussion Paper |

thickness of an ice dome in steady state depends on the regional accumulation rate average, the temperature of the ice, and the aerial extent of the dome (Bueler et al., 2005). For this estimate, we take the geologically defined aerial extent (Table 2) and assume a dome base of circular area that has the same area as the geologically defined dome. Figure 8 shows the results of our model with red ellipses defining the range of possible ice thickness values for each dome. The minor axis of the red ellipses shows a possible range of error in the ice radius associated to a slight over estimation effect. Because we lack specific data for LGM accumulation rate and ice temperature, we use our best guesses to bound the ice thicknesses and volumes as follows. For the modern AP, the western side has higher average temperatures than the eastern side suggesting that in the past, the ice domes on the western side will be warmer on average than the eastern side. We assume that the western-side domes (Marr, Livingston, Brabant, and Hugo) have an average ice temperature of 0 °C (Fig. 8a), while the eastern-side domes have an average ice temperature of −10 °C (Fig. 8b). The colder ice is stiff, this can result in larger domes if all other parameters are the same.

For accumulation rates, we base our assumptions on the modern AP, which has a strong orographic precipitation gradient that ranges from 4 $m\,yr^{-1}$ on the western side to less than 0.1 $m\,yr^{-1}$ on the eastern side. High accumulation sites will result in thicker ice domes if all other parameters are equal. In the LGM case, the distribution of domes will create multiple precipitation highs and lows as each dome creates its own pattern of orographic precipitation (Roe and Lindzen, 2001). Therefore we predict the highest accumulation rates for Brabant, Livingston, and Hugo Domes. Marr Dome will likely be shielded somewhat from the highest accumulation. On the eastern side, Hektoria and Snow Hill Domes are likely to have slightly higher accumulation than Robertson Dome, as they may receive some precipitation from the Weddell Sea. We have selected a broad range of accumulation rates because we have only general atmospheric patterns from which to draw our assumptions. Despite this large range of input values, we can bracket the ice thicknesses for each dome as presented in Fig. 8, and estimate volumes, as shown in Table 2.

4.4 Regional implications

We have presented a compilation of paleo-ice flow indicators for the northern AP and used the resulting map to infer ice flow patterns, ice divides and accumulation centers. This allows an integrated view over the full extent of the APIS at the LGM. This mapping effort suggests that the seabed topography and the complex geology influenced the ice flow route and regime at the LGM. The bifurcation of the flow lines in the Larsen-B embayment affected the character of the basal ice erosion mechanisms. In general, diverging ice flow is associated with an area of decelerating flow (e.g. Stokes and Clark, 2003). Moreover, the increased flux of ice and debris flowing around a topographic high could provide a powerful feed-back where ice stream could deepen existing depressions (Knight et al., 1994). On the other hand, the flow convergences (strongest near the mid-shelf in the northern AP) led to an increase in flow speed at the mid- and upper end of the ice streams, promoting high basal shear stress and significant basal sediment transport (e.g. Boulton, 1990).

The presence of multiple APIS ice domes centered on the mid-shelf implies that ice thickness was not uniform on the northern AP continental shelf during the maximum extension of the APIS at LGM. These domes may have harbored significant ice volume, even under minimal scenarios of ice thickness due to their large areal extent. Comparing the estimated total area of the ice domes with the one estimated for the flow paths (Tables 2 and 3) shows that the ice domes were at least as important if not more so than the paleo-ice streams, in terms of areal coverage. Our assumptions related to ice volumes estimates of the converging flow paths are not as strong as the ones we use for the ice domes. Because of this the minimum estimate for totals ice volume of the domes and the paleo-ice streams are similar. Because the convergent flow paths have significantly deeper beds (as they flow in troughs) the maximum total ice volume for the paleo ice streams is 27 085 km^3 more than the volume estimate for the ice dome system. The presence of multiple ice domes on the shelf would likely have controlled the ice sheet dynamics (e.g. basal melting and sliding parameters) and the sediment transport to the ocean (shelf break). The ice velocity would have been slower near the ice divides with lower sediment transport rates than at the peripheral regions where the domes fed out into fast flowing ice streams with high sediment transport rates. Because of feedbacks between ice dome formation and the orographic precipitation, all of these domes may not have reached their largest extent at the same time; the growth of one dome may “starve” another of its accumulation (e.g. Roe and Lindzen, 2001).

Finally, the delineation of ice domes and faster flowing outlets is important in that it would help to gauge the relative contribution of each system to post glacial eustatic rise in sea level or conversely how each system might have responded to a eustatic or ocean-climate event. For instance, recent models for glacial recession within the Palmer Deep and along the East Antarctic margin suggest a calving bay re-entrant model, wherein ice streams retreat preferentially landward thus creating a linear “fjord” like bay surrounded by slower flowing ice of the domes (Domack et al., 2006; Leventer et al., 2006). This model deserves consideration in that our reconstruction clearly outlines differences in the boundary conditions of flow, thickness, bed character, accumulation, and ice sourcing for the domes and converging flow systems. Thus the two systems would logically be expected to respond differently to any forcing factors involved in deglaciation.

The identification of ice domes, ice-drainage divides and diverging/converging flows help us to understand ice-sheet evolution and processes. These features have important implications for the future siting of ice cores and marine drilling sites. Finally, they provide important constraints for glaciohydrology, past and future ice sheet flow modeling to provide more realistic predictions, ice sheet modeling in response to changing environments, and sea level modeling. While the evidence for the ice domes out on the shelf is in large part circumstantial; there exists today likely remnants to these features as is the case for the ice cap on Hugo Island, where it stands as a prominent feature in the middle of the Antarctic Peninsula continental shelf.

5 Conclusions

Our results provide considerable improvement in the assessment of ice flow and thereby the dynamics that may have governed expansion, stabilization and eventual demise of the ice mass which comprised the APIS. We now recognize not only six spatially defined paleo-ice streams but can infer with some confidence the source areas and number of tributaries which fed them. In addition, our study highlights the need to understand the extent and behavior of seven large ice domes that we now infer for the continental shelf where these ice masses were supported by local accumulation and served as lateral constraints to paleo-ice stream flow. These ice domes had slower flowing ice and may have been frozen to their beds, exhibiting somewhat different behavior to the paleo-ice streams which were fed almost exclusively from convergence of tributary glaciers draining the elevated spine of the AP and surrounding islands. Also, while the timing of paleo-ice stream recession is known in a general way from recent syntheses (Ó Cofaigh et al., 2014) the detailed rates and step backs are far from resolved. Our reconstruction allows focus upon the varying character of each ice stream and how this might have influenced differential response to the forcing factors (i.e. eustasy, atmospheric and ocean temperature) and accumulation rates which may have induced instability in the region.

Future research including more multibeam coverage, marine sediment cores and modeling considering the glacio-isostatic rebound are needed to confirm the existence of the ice domes, define their characteristics and constrain the timing of ice retreat from them. When combined with high resolution dating efforts, our flow reconstruction will help elucidate the retreat history of the ice sheet, and, therefore, those forces that acted to destabilize the system and initiate the most recent de-glaciation of the APIS.

The Supplement related to this article is available online at doi:10.5194/tcd-8-5321-2014-supplement.

Discussion Paper | Discussion Paper | Discussion Paper | Discussion Paper |

Acknowledgements. This work was funded by U.S. National Science Foundation grants OPP-0732467 to Eugene W. Domack, ANT-1340261 and ANT-0732921 to Ted Scambos, and OPP-0855265 to Erin C. Pettit, and the Korean Polar Research Institute (PP14010). In addition, we thank the captains and crews of the RVIB Nathaniel B. Palmer, Polarstern, RRS James Clark Ross, BIO Hesperides, and Aaron, and support staffs and scientific parties who participated in cruises. This work contains public sector information, licensed under the Open Government Licence v2.0, from the UK Hydrographic Office for the data collected on HMS Endurance, HMS Scott and HMS Protector. All Principal investigators owner of the released swath multibeam data from the Marine Geoscience Data System portal hosted by Lamont-Doherty Earth Observatory of Columbia University (http://www.marine-geo.org/index.php). C. Lavoie was supported by "TALENTS" Marie Curie COFUND FP7 Programme and MARES programme and an individual Research Assistant contract within the project MARES-Sustainable Use of Marine Resources (CENTRO-07-ST24-FEDER-002033), co-financed by QREN, Mais Centro – Programa Operacional Regional do Centro e União Europeia/European Regional Development Fund (EU).

References

Amblas, D., Urgeles, R., Canals, M., Calafat, A. M., Robesco, M., Camerlenghi, A., Estrada, F., De Batist, M., and Hughes-Clarke, J. E.: Relationship between continental rise development and palaeo-ice sheet dynamics, Northern Antarctic Peninsula Pacific margin, Quaternary Sci. Rev., 25, 933–944, 2006.

Andrews, J. T.: On the reconstitution of pleistocene ice sheets: a review, Quaternary Sci. Rev., 1, 1–30, 1982.

Arndt, J. E., Schenke, H. W., Jakobsson, M., Nitsche, F. O., Buys, G., Goleby, B., Rebesco, M., Bohoyo, F., Hong, J., Black, J., Greku, R., Udintsev, G., Barrios, F., Reynoso-Peralta, W., Taisei, M., and Wigley, R.: The International Bathymetric Chart of the Southern Ocean (IBCSO) Version 1.0 – a new bathymetric compilation covering circum-Antarctic waters, Geophys. Res. Lett., 40, 3111–3117, 2013.

Banfield, L. A. and Anderson, J. B.: Seismic facies investgation of the late Quaternary glacial history of Bransfield Basin, Antarctica, in: Geology and Seismic Stratigraphy of the Antarctic Margin, edited by: Cooper, A. K., Barker, P. F., and Brancolini, G., Antarct. Res. Ser. 68, American Geophysical Union, Washington, D.C., 123–140, 1995.

Bentley, M. J. and Anderson, J. B.: Glacial and marine geological evidence for the ice sheet configuration in the Weddell Sea-Antarctic Peninsula region during the Last Glacial Maximum, Antarct. Sci., 10, 309–325, 1998.

Boulton, G. S.: Sedimentary and sea level changes during glacial cycles and their control on glacimarine facies architecture. in: Glacimarine Environments: Processes and Sediments, edited by: Dowdeswell, J. A. and Scourse, J. D., Geological Society Special Publication 53, The Geological Society, London, 15–52, 1990.

Brisbourne, A. M., Smith, A. M., King, E. C., Nicholls, K. W., Holland, P. R., and Makinson, K.: Seabed topography beneath Larsen C Ice Shelf from seismic soundings, The Cryosphere, 8, 1–13, doi:10.5194/tc-8-1-2014, 2014.

Bueler, E., Lingle, C. S., Kallen-Brown, J. A., Covey, D., and Bowman, L. N.: Exact solutions and verification of numerical models for isothermal ice sheets, J. Glaciol., 51, 291–306, 2005.

Camerlenghi, A., Domack, E. W., Rebesco, M., Gilbert, R., Ishman, S., Leventer, A., Brachfeld, S., and Drake, A.: Glacial morphology and post-glacial contourites in northern Prince Gustav Channel (NW Weddell Sea, Antarctica), Mar. Geophys. Res., 22, 417–443, 2001.

Canals, M., Urgeles, R., and Calafat, A. M.: Deep sea-floor evidence of past ice streams off the Antarctic Peninsula, Geology, 28, 31–34, 2000.

Canals, M., Casamor, J. L., Urgeles, R., Calafat, A. M., Domack, E. W., Baraza, J., Farran, M., and De Batist, M.: Seafloor evidence of a subglacial sedimentary system off the northern Antarctic Peninsula, Geology, 30, 603–606, 2002.

Canals, M., Calafat, A. M., Camerlenghi, A., De Batist, M., Urgeles, R., Farran, M., Geletti, R., Versteeg, W., Amblas, D., Rebesco, M., Casamor, J. L., Sànchez, A., Willmott, V., Lastras, G., and Imbo, Y.: Uncovering the footprint of former ice streams off Antarctica, EOS, 84, 97–108, 2003.

Clark, C. D.: Mega-sclae glacial lineations and cross-cutting ice-flow landforms, Earth Surf. Proc. Land., 18, 1–29, 1993.

Clark, C. D., Tulaczyk, S., Stokes, C. R., and Canals, M.: A groove-ploughing theory for the production of mega-scale glacial lineations, and implications for ice-stream mechanics, J. Glaciol., 49, 240–256, 2003.

Conway, H., Catania, G., Raymond, C. F., and Gades, A. M.: Switch of flow direction in an Antarctic ice stream, Nature, 419, 465–467, 2002.
Curry, P. and Pudsey, C. J.: New Quaternary sedimentary records from near the Larcen C and former Larsen B ice shelves; evidence for Holocene stability, Antarct. Sci., 19, 355–364, 2007.
Davies, B. J., Hambrey, M. J., Smellie, J. L., Carrivick, J. L., and Glasser, N. F.: Antarctic Peninsula Ice Sheet evolution during the Cenozoic Era, Quaternary Sci. Rev., 31, 30–66, 2012.
Domack, E., Duran, D., Leventer, A., Ishman, S., Doane, S., McCallum, S., Amblas, D., Ring, J., Gilbert, R., and Prentice, M.: Stability of the Larsen B ice shelf on the Antarctic Peninsula during the Holocene epoch, Nature, 436, 681–685, 2005.
Domack, E., Amblas, D., Gilbert, R., Brachfeld, S., Camerlenghi, A., Robesco, M., Canals, M., and Urgeles, R.: Subglacial morphology and glacial evolution of the Palmer deep outlet system, Antarctic Peninsula, Geomorphology, 75, 125–142, 2006.
Dowdeswell, J. A., Ottesen, D., Evans, J., Ó Cofaigh, C., and Anderson, J. B.: Submarine glacial landforms and rates of ice-stream collapse, Geology, 26, 819–822, 2008.
Eittreim, S. L., Cooper, A. K., and Wannesson, J.: Seismic stratigraphic evidence of ice-sheet advances on the Wilkes Land margin of Antarctica, Sediment. Geol., 96, 131–156, 1995.
Evans, J., Dowdeswell, J. A., and Ó Cofaigh, C.: Late Quaternary submarine bedforms and ice-sheet flow in Gerlache Strait and on the adjacent continental shelf, Antarctic Peninsula, J. Quaternary Sci., 19, 397–407, 2004.
Evans, J., Pudsey, C. J., Ó Cofaigh, C., Morris, P., and Domack, E. W.: Late Quaternary glacial history, flow dynamics and sedimentation along the eastern margin of the Antarctic Peninsula Ice Sheet, Quaternary Sci. Rev., 24, 741–774, 2005.
Fretwell, P., Pritchard, H. D., Vaughan, D. G., Bamber, J. L., Barrand, N. E., Bell, R., Bianchi, C., Bingham, R. G., Blankenship, D. D., Casassa, G., Catania, G., Callens, D., Conway, H., Cook, A. J., Corr, H. F. J., Damaske, D., Damm, V., Ferraccioli, F., Forsberg, R., Fujita, S., Gim, Y., Gogineni, P., Griggs, J. A., Hindmarsh, R. C. A., Holmlund, P., Holt, J. W., Jacobel, R. W., Jenkins, A., Jokat, W., Jordan, T., King, E. C., Kohler, J., Krabill, W., Riger-Kusk, M., Langley, K. A., Leitchenkov, G., Leuschen, C., Luyendyk, B. P., Matsuoka, K., Mouginot, J., Nitsche, F. O., Nogi, Y., Nost, O. A., Popov, S. V., Rignot, E., Rippin, D. M., Rivera, A., Roberts, J., Ross, N., Siegert, M. J., Smith, A. M., Steinhage, D., Studinger, M., Sun, B., Tinto, B. K., Welch, B. C., Wilson, D., Young, D. A., Xiangbin, C., and Zirizzotti, A.:

Bedmap2: improved ice bed, surface and thickness datasets for Antarctica, The Cryosphere, 7, 375–393, doi:10.5194/tc-7-375-2013, 2013.
Gades, A., Raymond, C. F., Conway, H., and Jacobel, R.: Bed properties of Siple Dome and adjacent ice streams, West Antarctica, inferred from radio-echo sounding measurements, J. Glaciol., 46, 88–94, 2000.
Gilbert, R., Domack, E. W., and Camerlenghi, A.: Deglacial history of the Greenpeace Trough: ice Sheet to Ice Shelf transition in the Northwestern Weddell Sea, Antarct. Res. Ser., 79, 195–204, 2003.
Glasser, N. F., Davies, B. J., Carrivick, J. L., Rodés, A., Hambrey, M. J., Smellie, J. L., and Domack, E.: Ice-stream initiation, duration and thinning on James Rosse Island, northern Antarctic Peninsula, Quaternary Sci. Rev., 86, 78–88, 2014.
Graham, A. G. C. and Smith, J. A.: Palaeoglaciology of the Alexander Island ice cap, western Antarctic Peninsula, reconstructed from marine geophysical and core data, Quaternary Sci. Rev., 35, 63–81, 2012.
Heroy, D. C. and Anderson, J. B.: Ice-sheet extent of the Antarctic Peninsula region during the Last Glacial Maximum (LGM) – insights from glacial geomorphology, Geol. Soc. Am. Bull., 117, 1497–1512, 2005.
Heroy, D. C., Sjunneskog, C., and Anderson, J. B.: Holocene climate change in the Bransfield Basin, Antarctic Peninsula: evidence from sediment and diatom analysis, Antarct. Sci., 20, 69–87, 2008.
Johnson, J. S., Bentley, M. J., Roberts, S. J., Binnie, S. A., and Freeman, S. P. H. T.: Holocene deglacial history of the northeast Antarctic Peninsula – a review and new chronological constraints, Quaternary Sci. Rev., 30, 3791–3802, 2011.
Joughin, I., Fahnestock, M., MacAyeal, D. R., Bamber, J. L., and Gogineni, P.: Observation and analysis of ice flow in the largest Greenland ice stream, J. Geophys. Res., 106, 34021–34034, 2001.
Joughin, I., Smith, B. E., Howat, I. M., Scambos, T., and Moon, T.: Greenland flow variability from ice-sheet-wide velocity mapping, J. Glaciol., 56, 415–430, 2010.
Knight, P. G., Sugden, D. E., and Minty, C. D.: Ice flow around large obstacles as indicated by basal ice exposed at the margin of the Greenland ice sheet, J. Glaciol., 40, 359–367, 1994.
Larter, R. D. and Barker, P. F.: Seismic stratigraphy of the Antarctic Peninsula Pacific margin: a record of Pliocene–Pleistocene ice volume and paleoclimate, Geology, 17, 731–734, 1989.

Larter, R. D. and Vanneste, L. E.: Relict subglacial deltas on the Antarctic Peninsula outer shelf, Geology, 23, 33–36, 1995.
Lawver, L. A., Sloan, B. J., Barker, D. H. N., Ghidella, M. E., von Herzen, R. P., Keller, R. A., Klinkhammer, G. P., and Chin, C. S.: Distributed, active extension in Bransfield Basin, Antarctic Peninsula: evidence from multibeam bathymetry, GSA Today, 6, 1–6, 1996.
Leventer, A., Domack, E., Dunbar, R., Pike, J., Stickley, C., Maddison, E., Brachfield, S., Manely, P., and McClennan, C.: Marine sediment record from East Antarctica margin reveals dynamics of ice-sheet recession, GSA Today, 16, 4–10, 2006.
Livingstone, S. J., Ó Cofaigh, C., Stokes, C. R., Hillenbrand, C. D., Vieli, A., and Jamieson, S. S. R.: Antarctic palaeo-ice streams, Earth-Sci. Rev., 111, 90–128, 2012.
Marshall, S. J. and Cuffey, K. M.: Peregrinations of the Greenland Ice Sheet divide in the last glacial cycle: implications for central Greenland ice cores, Earth Planet. Sc. Lett., 179, 73–93, 2000.
Nereson, N. A., Hindmarsh, R. C. A., and Raymond, C. F.: Sensitivity of the divide position at Siple Dotne, West Antarctica, to boundary forcing, Ann. Glaciol., 27, 207–214, 1998.
Ó Cofaigh, C., Davies, B. J., Livingstone, S. J., Smith, J. A., Johnson, J. S., Hocking, E. P., Hodgson, D. A., Anderson, J. B., Bentley, M. J., Canals, M., Domack, E., Dowdeswell, J. A., Evans, J., Glasser, N. F., Hillenbrand, C. D., Larter, R. D., Roberts, S. J., and Simms, A. R.: Reconstruction of ice-sheet changes in the Antarctic Peninsula since the Last Glacial Maximum, Quaternary Sci. Rev., 100, 87–110, 2014.
Pudsey, C. J., Barker, P. F., and Larter, R. D.: Ice Sheet retreat from the Antarctic Peninsula shelf, Cont. Shelf. Res., 14, 1647–1675, 1994.
Pudsey, C. J., Evans, J., Domack, E. W., Morris, P., and Del Valle, R. A.: Bathymetry and acoustic facies beneath the former Larsen-A and Prince Gustav ice shelves, north-west Weddell Sea, Antarct. Sci., 13, 312–322, 2001.
Rebesco, M., Liu, Y., Camerlenghi, A., Winsborrow, M., Laberg, J. S., Caburlotto, A., Diviacco, P., Accettella, D., Sauli, C., Wardell, N., and Tomini, I.: Deglaciation of the western margin of the Barents Sea Ice Sheet – a swath bathymetric and sub-bottom seismic study from the Kveithola Trough, Mar. Geol., 279, 141–147, 2011.
Reinardy, B. T. J., Larter, L. D., Hillenbrand, C. D., Murray, T., Hiemstra, J. F., and Booth, A. D.: Streaming flow of an Antarctic Peninsula palaeo-ice stream, both by basal sliding and deformation of substrate, J. Glaciol., 57, 596–608, 2011.

Roe, G. H. and Lindzen, R. S.: The mutual interaction between continental-scale ice sheets and atmospheric stationary waves, J. Climate, 14, 1450–1465, 2001.
Scambos, T. A., Hulbe, C. L., and Fahnestock, M.: Climate-induced ice shelf deisintegration in the Antarctic Peninsula, in: Antarctic Peninsula Climate Variability, edited by: Domack, E. W., Leventer, A., Burnett, A., Bindschadler, R., Convey, P., and Kirby, M., Antarct. Res. Ser. 79, American Geophysical Union, Washington, D.C., 79–92, 2003.
Simms, A. R., Milliken, K. T., Anderson, J. B., and Wellner, J. S.: The marine record of deglaciation of the SouthShetlandIslands, Antarctica since the Last Glacial Maximum, Quaternary Sci. Rev., 30, 1583–1601, 2011.
Sloan, B. J., Lawver, L. A., and Anderson, J. B.: Seismic stratigraphy of the Larsen Basin Eastern Antarctic Peninsula, in: Geology and Seismic Stratigraphy of the Antarctic Margin, edited by: Cooper, A. K., Barker, P. F., and Brancolini, G., Antarctic Res. Ser. 68, American Geophysical Union, Washington, D.C., 59–74, 1995.
Smith, R. T. and Anderson, J. B.: Ice-sheet evolution in James Ross Basin, Weddell Sea margin of the Antarctic Peninsula: the seismic stratigraphic record, Geol. Soc. Am. Bull., 122, 830–842, 2009.
Smith, T. and Anderson, J. B.: Seismic stratigraphy of the Joinville Platform: implications for regional climate evolution, in: Tectonic, Climatic and Cryospheric Evolution of the Antarctic Peninsula, edited by: Anderson, J. B. and Wellner, J. K., American Geophysical Union Special Publication 063, American Geophysical Union, Washington, D.C., 51–62, 2011.
Stokes, C. R. and Clark, C. D.: The Dubawnt Lake palaeo-ice stream: evidence for dynamic ice sheet behaviour on the Canadian Shield and insights regarding the controls on ice-stream location and vigour, Boreas, 32, 264–279, 2003.
Vanneste, L. E. and Larter, R. D.: Deep-tow boomer survey on the Antarctic Peninsula Pacific Margin: an investigation of the morphology and acoustic characteristics of Late Quaternary sedimentary deposits on the outer continental shelf and upper slope, in: Geology and Seismic Stratigraphy of the Antarctic Margin, Part 1, edited by: Cooper, A. K., Barker, P. F., and Brancolini, G., American Ggophysical Union, Washington, D.C., 97–121, 1995.
Wellner, J. S., Lowe, A. L., Shipp, S. S., and Anderson, J. B.: Distribution of glacial geomorphic features on the Antarctic continental shelf and correlation with substrate: implications for ice behavior, J. Glaciol., 47, 397–411, 2001.

Discussion Paper | Discussion Paper | Discussion Paper | Discussion Paper |

Wellner, J. S., Heroy, D. C., and Anderson, J. B.: The death mask of the antarctic ice sheet: comparison of glacial geomorphic features across the continental shelf, Geomorphology, 75, 157–171, 2006.

Willmott, V., Canals, M., and Casamor, J. L.: Retreat history of the Gerlache–Boyd ice stream, Northern Antarctic Peninsula: an ultra-high resolution acoustic study of the deglacial and post-glacial sediment drape, in: Antarctic Peninsula Climate Variability, edited by: Domack, E. W., Leventer, A., Burnett, A., Bindschadler, R., Peter, C., and Kirby, M., Antarct. Res. Ser., 79, 183–194, 2003.

Table 1. Reef and shoal areas in the northwestern Weddell Sea*.

Latitude	Longitude	Notes
65.237° S 65.183° S	59.251° W to 58.213° W	"Robertson reef", 49 km long, bearing 005° numerous high points, shallow depth (est. ~ 100 m depth)
66.912° S 66.813° S	60.133° W to 59.468° W	"Bawden reef", extending 34 km from s. end of ice rise, arcuate, bearing 020° numerous high points, shallow depth (est. ~ 100 m depth)
66.174° S 66.177° S 66.025° S	58.968° W w 58.721° W e 58.806° W n	"Jason shoals", 12 km × 18 km region, 3–4 high points; shallow depth at west end (est. 100–150 m depth)
65.784° S	58.237° W	"Hektoria 1 shoal", single point (est. > 150 m depth)
65.849° S	57.276° W	"Hektoria 2 shoal", single point (est. > 150 m depth)
65.692° S	56.956° W	"Hektoria 3 shoal", single point (est. > 150 m depth)
66.292° S	56.975° W	"Hektoria 4 shoal", single point (est. > 150 m depth)

* Based on sea ice and small iceberg strand sites, and winter sea ice fracture loci, seen in MODIS image data archived at http://nsidc.org/data/iceshelves_images/index_modis.html.

Table 2. Continental shelf domes estimated area, and minimum and maximum estimated ice volumes using the simple Bodvarsson-vialov model (Bueler et al., 2005).

Continental Ice Dome	Area (km^2)	Ice volume (km^3)	
		Minimum	Maximum
Hugo Dome	13 675	10 000	11 200
Marr Dome	4950	2500	3300
Brabant Dome	12 850	8200	10 200
Livingston Dome	8075	5000	5500
Snow Hill Dome	14 835	10 800	14 000
Robertson Dome	7560	5000	6200
Hektoria Dome	12 920	9300	12 000
TOTAL	74 865	50 800	62 400

Table 3. Flow path systems estimated area, and minimum and maximum estimated ice volumes.

Flow Path System	Area (km^2)	Approximate length (km)	Ice volume (km^3)	
			Minimum	Maximum
Biscoe Trough	4625	125	2842	4254
Palmer Deep and hugo Island Trough	15 000	230	9570	17 255
Barbant	850	60	564	719
Gerlache–Croker–Boyd Straits	10 675	300	9234	16 402
South Bransfield Strait streams	5600	110	4211	5834
Erebus-Terror	7125	190	3905	6935
Robertson Trough	18 300	330	13 066	26 149
Larsen B embayment	10 700	217	6736	11 937
TOTAL	72 875	1562	50 128	89 485

Discussion Paper | Discussion Paper | Discussion Paper | Discussion Paper |

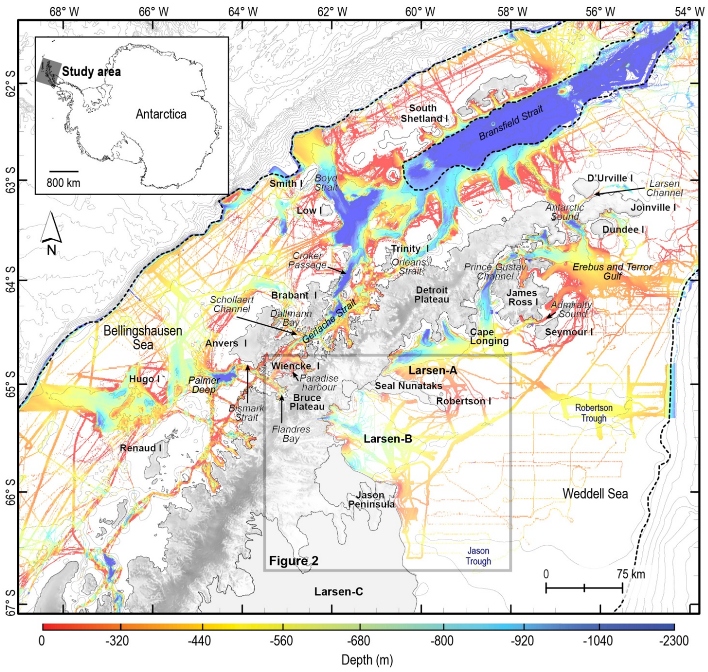

Figure 1. Location map and details of the swath bathymetry data base, as compiled up to 2013, around the northern Antarctic Peninsula (AP). Offshore topography is gridded at 30 m. The shelf break is shown as a black dashed line. The grey box indicates the regions detailed in Fig. 2. The background image on land is from RAMP AMM-1 SAR Image 125 m Mosaic of Antarctica; the coastline from the British Antarctic Survey (BAS; http://www.add.scar.org/); the bathymetry contour interval of 250 m is from IBCSO (Arndt et al., 2013). The inset shows the location of the northern AP in Antarctica.

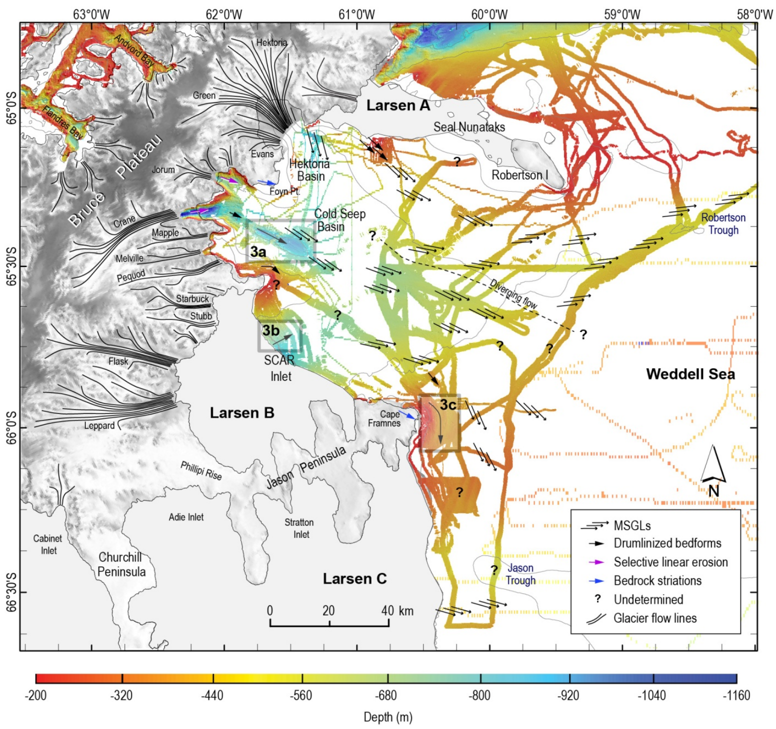

Figure 2. Details of seabed morphology in Larsen-B embayment associated with paleo-flow line trajectories based upon examination of swath bathymetry imagery of the seafloor. Distinct flow trajectories which split the Larsen-B embayment into two outlets by ice flow bifurcation. The bathymetry contour interval of 250 m is from IBCSO (Arndt et al., 2013). The gray boxes show the regions detailed in Fig. 3. For location see Fig. 1.

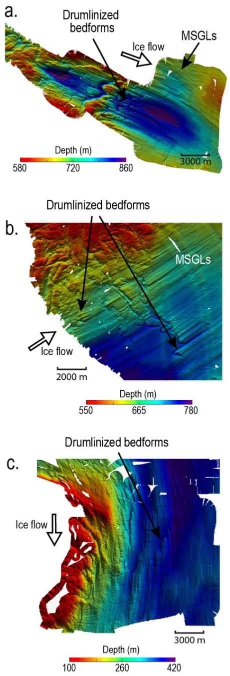

Figure 3. Close-up on the seabed morphology and swath bathymetry perspective views. The location of **(a)**–**(c)** is presented in Fig. 2. Offshore topography is gridded at 25 m and showed with a vertical exaggeration of X3 **(a)** Bathymetry image showing the Cold Seep Basin region with drumlinized bedforms and Mega Scale Glacial Lineations (MSGLs) associated to a paleo-ice flow direction, **(b)** SCAR Inlet, and **(c)** Cape Framnes, south of the Jason Peninsula. The paleo-ice flow direction is indicated by the white narrow.

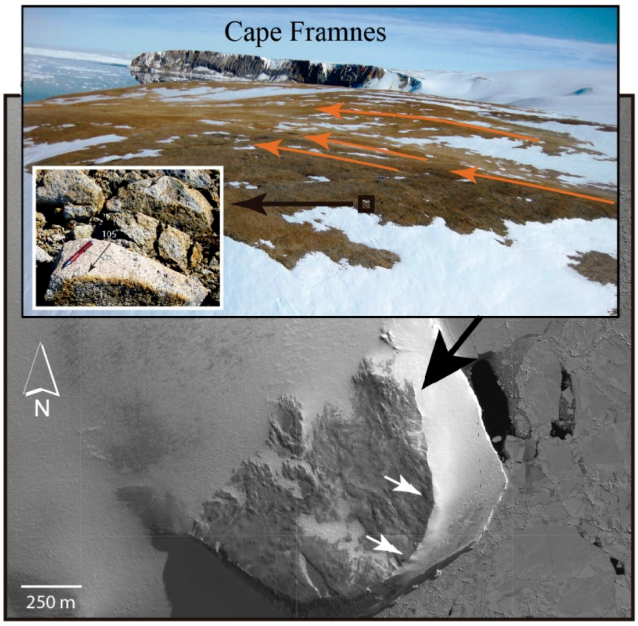

Figure 4. Photography from Cape Framnes showing bedrock striations and flute orientations SSW in agreement with the southward flow orientation observed on the seafloor (this study). The location of the photograph and its aspect is indicated by the black arrow on the Landsat Scenes LIMA. The insets show an isolated bedrock rib, its location on the landscape and the flow direction of striations and bedrock flutes (orange and white arrows) in each case, respectively (figure modified from a map compiled by Spences Niebuhr, Polar Geospatial Center).

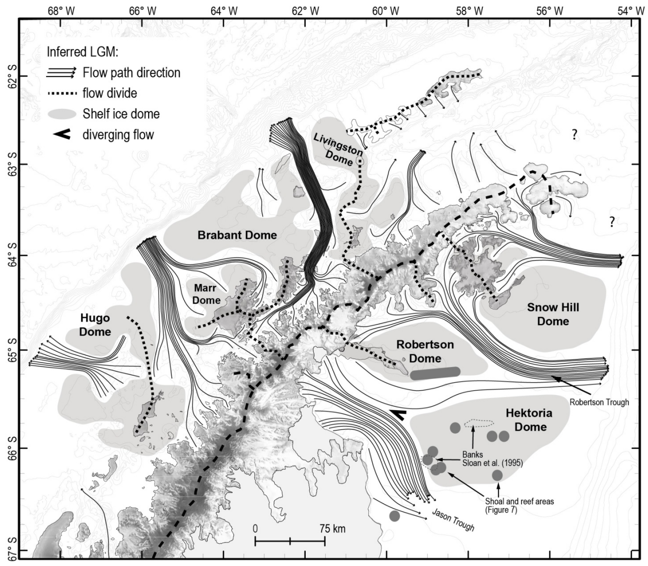

Figure 5. Inferred paleo-ice flow directions and continental shelf ice domes around the northern AP continental shelf at LGM showing ice divides (black short-dashed lines), shelf ice domes (gray areas) and the bifurcating flow in the Larsen-B embayment. The modern divide along the AP (black dash line) is probably not at the same location of the LGM divide, but close. Also identified the topographic banks by Sloan et al. (1995) and the shoal and reef areas of Fig. 7. The bathymetry contour interval of 250 m is from IBCSO (Arndt et al., 2013).

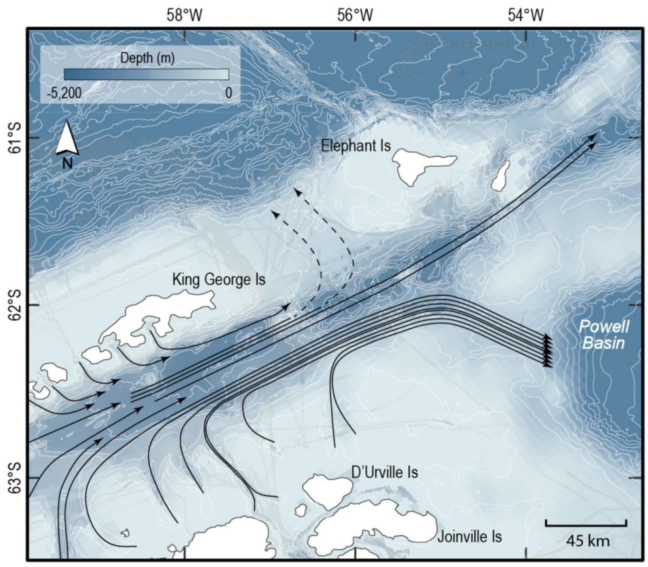

Figure 6. Seabed morphology in Bransfield Strait showing the inferred paleo-flow line trajectories based upon the multibeam imagery (black arrows) and assumptions (black dashed arrows). Background image is from BedMap2 (Fretwell et al., 2013); the islands coastline from the British Antarctic Survey (BAS; http://www.add.scar.org/); the bathymetry contour interval of 250 m is from IBCSO (Arndt et al., 2013).

Discussion Paper | Discussion Paper | Discussion Paper | Discussion Paper |

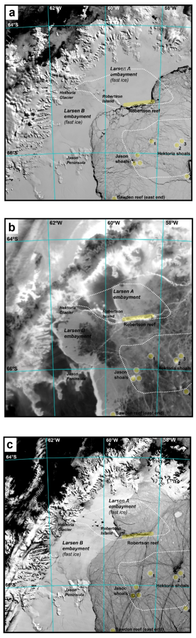

Figure 7. MODerate-resolution Imaging Spectroradiometer (MODIS, 36 band spectrometer) images showing unequivocal evidence of several shoal and reef areas (yellow circle) in the northwestern Weddell Sea, based on sea ice drift and grounding of small icebergs (see also Table 1). The shelf ice domes Hektoria and Robertson are showed in dashed white line. **(a)** 5 October 2007, Band Number (BN) 02 (bandwidth 841–876 nm, spatial resolution of 250 m), **(b)** 20 August 2010, BN 32 (bandwidth 11 770–12 270 nm, spatial resolution of 1000 m) and **(c)** 26 January 2013, BN 02 (bandwidth 841–876 nm, spatial resolution of 250 m).

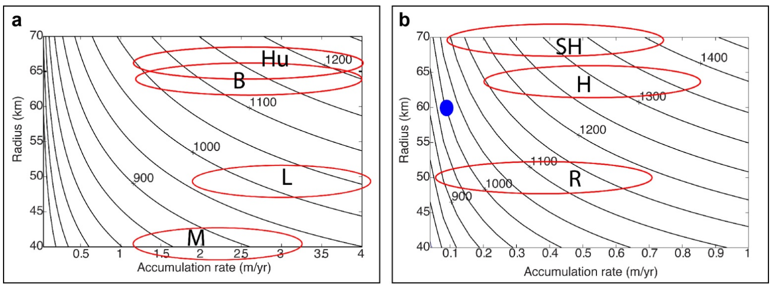

Figure 8. Range of ice thickness expected from **(a)** Marr (M), Livingston (L), Brabant (B), and Hugo (Hu) west AP continental-shelf domes where the ice temperature is assumed to average 0 °C, and **(b)** Robertson (R), Hektoria (H), and Snow Hill (SH) east AP continental-shelf domes with ice averaging −10 °C using the Bodvarsson–Vialov model (Bueler et al., 2005). The blue dot is the modern analog Siple Dome in West Antarctica of 1000 m thick that fits well the model. See Fig. 5 for the location of the domes.